Available online at www.sciencedirect.com

SciVerse ScienceDirect

Journal of Nutritional Biochemistry 24 (2013) 146–155

Journal of Nutritional Biochemistry

Attenuation of high-glucose-induced inflammatory response by a novel curcumin derivative B06 contributes to its protection from diabetic pathogenic changes in rat kidney and heart☆

Yong Pan[a,1], Guanghui Zhu[b,1], Yi Wang[a], Lu Cai[a,c], Yuepiao Cai[a], Jie Hu[a], Yilan Li[a], Yongbo Yan[a], Zengshou Wang[b], Xiaokun Li[a], Tiemin Wei[d,*], Guang Liang[a,*]

[a]School of Pharmaceutical Science, Wenzhou Medical College, Wenzhou, People's Republic of China
[b]Department of Pharmacy, The 2nd Affiliated Hospital, Wenzhou Medical College, Wenzhou, People's Republic of China
[c]Department of Pediatrics, University of Louisville, Louisville, KY, USA
[d]The 5nd Affiliated Hospital, Wenzhou Medical College, Wenzhou, People's Republic of China

Received 23 October 2011; received in revised form 2 February 2012; accepted 7 March 2012

Abstract

There is increasing evidence indicating that inflammatory processes are involved in the development and progression of diabetic complications. However, effective anti-inflammatory treatments for patients who have diabetic complications have yet been practically identified. Curcumin is a main component of *Curcuma longa* with numerous pharmacological activities. Previously, we synthesized a novel curcumin analogue (B06) that exhibited an improved pharmacokinetic and enhanced anti-inflammatory activity compared to curcumin. The present study aimed to test the hypothesis that B06 may reduce high-glucose-induced inflammation and inflammation-mediated diabetic complications. *In vitro*, pretreatment with B06 at a concentration of 5 μM significantly reduced the high-glucose-induced overexpression of inflammatory cytokines in macrophages. This anti-inflammatory activity of B06 is associated with its inhibition of c-Jun N-terminal kinase/nuclear factor κB activation. *In vivo*, despite that B06 administration at 0.2 $mg \cdot kg^{-1} \cdot d^{-1}$ for 6 weeks did not affect the blood glucose profile of diabetic rats, the B06-treated animals displayed significant decreases in inflammatory mediators in the serum, kidney, and heart and renal macrophage infiltration. This was accompanied with an attenuation of diabetes-induced structural and functional abnormalities in the kidney and heart. Taken together, these data suggest that the novel derivative B06 might be a potential therapeutic agent for diabetic complications via an anti-inflammatory mechanism and support the potential application in diabetic complication therapy via anti-inflammatory strategy.

Keywords: (1*E*,4*E*)-1,5-bis(2-bromophenyl)penta-1,4-dien-3-one; Anti-inflammation; High glucose; Diabetic complication; Macrophage

1. Introduction

In recent years, the concept that an interplay between inflammatory and metabolic abnormalities leads to tissue damage in diabetes has been widely accepted [1]. There is considerable experimental evidence that proinflammatory and adhesion molecules are important in the development of diabetic complications [1–3]. Inflammatory mediators activate a series of receptors, leading to β-cell dysfunction and apoptosis, insulin signaling impairment, systemic endothelial dysfunction, and altered vascular flow, which constitute final common pathways to the vascular complications of diabetes [1–4]. Several studies have shown that inflammation directly caused heart and kidney damage in streptozotocin (STZ)-induced animals, leading to diabetic cardiomyopathy and nephropathy [1,3–5]. The manifestations of this inflammatory state include nuclear factor (NF)-κB-dependent overproduction of inflammatory mediators such as tumor necrosis factor (TNF)-α, interleukin-6 (IL-6), IL-1β, cyclooxygenase (COX)-2, inducible nitric oxide synthase (iNOS), transforming growth factor (TGF)-β, and monocyte chemoattractant protein (MCP)-1 in the hearts and kidneys of diabetic rats [3–7]. Therefore, agents that attenuate the inflammatory response may be useful in medical management or prevention of patients with diabetic complications [2,8].

☆ Authorship contributions: Participated in research design: Lu Cai, Xiaokun Li, Tiemin Wei, and Guang Liang. Conducted experiments: Yong Pan, Yi Wang, Congcong Yu, Jianling Li, Guanghui Zhu, and Yilan Li. Contributed new reagents or analytic tools: Jie Hu, Zengshou Wang, and Yongbo Yan. Performed data analysis: Yong Pan, Guanghui Zhu, Yi Wang, Yuepiao Cai, and Guang Liang. Wrote or contributed to the writing of the manuscript: Yong Pan, Guanghui Zhu, Lu Cai, and Guang Liang.

* Corresponding authors. Bioorganic and Medicinal Chemistry Research Center, School of Pharmaceutical Science, Wenzhou Medical College, Wenzhou 325035, China. Tel.: +86 577 86699892; fax: +86 577 86689983.
E-mail addresses: lswtm@sina.com (T. Wei), wzmcliangguang@163.com (G. Liang).

[1] These authors contribute equally to this study.

0955-2863/$ - see front matter © 2013 Elsevier Inc. All rights reserved.
http://dx.doi.org/10.1016/j.jnutbio.2012.03.012

Curcumin is a hydrophobic polyphenol derived from the rhizome of the herb *Curcuma longa*. It has shown a variety of biological and pharmacological activities including anti-inflammatory, antioxidative, anticarcinogenic, and anti-infectious activities [9,10]. Chiu et al. [11] reported that curcumin is effective in preventing glucose-induced oxidative stress in the endothelial cells and hearts of diabetic animals. It has also been shown that short-term treatment with curcumin prevents diabetes-induced decreased antioxidant enzyme levels and kidney dysfunction in diabetic rats [12]. In addition, various studies in animal models and humans have confirmed that dietary curcumin is extremely safe and does not cause hazardous effects, even at high dosages [13]. Although curcumin is remarkably nontoxic and exerts a therapeutic potential in diabetic cardiomyopathy and nephropathy, its clinical application has been significantly limited by its instability *in vitro* and poor pharmacokinetic profiles *in vivo* [13–15]. Thus, development of synthetic structural analogues of curcumin is one approach for overcoming the poor bioavailability while retaining, or further enhancing, its drug-like effects [16,17]. In the previous studies, we designed and synthesized a series of curcumin analogues with improved pharmacokinetic profiles *in vivo* [18]. In these analogues, a novel compound (1*E*,4*E*)-1,5-bis(2-bromophenyl)penta-1,4-dien-3-one (B06; coded as B33 previously [18]) was found to possess a plasma amount that was approximately 44 times as great as that of curcumin (area under the curve) and a peak blood concentration of approximately 45 times that of curcumin [18]. In addition, this molecule exhibited a significant IL-6-inhibitory property in lipopolysaccharide (LPS)-stimulated mouse J774A.1 macrophages (coded as B03 there) [19]. Thus, we hypothesized that B06 is able to reduce high-glucose (HG)-induced inflammation, thereby preventing diabetic complications at a relatively low dosage. In the present study, we proved the ability of B06, even at an extremely low dosage (0.2 $mg \cdot kg^{-1} \cdot d^{-1}$), to significantly prevent diabetes-induced renal and cardiac inflammation and their pathological damages. Also, we showed that the protective mechanism of B06 was mediated by inhibiting c-Jun N-terminal kinase (JNK)/NF-κB activation. Thus, our finding suggests that B06, the novel curcumin analogue that has an improved pharmacokinetic profile, may be beneficial in patients with chronic diabetic complications.

2. Methods and materials

2.1. Reagents

Glucose and mannitol were purchased from Sigma (Louis, MO, USA). Curcumin analogue B06 was prepared with a purity of 99.2% as described in our previous study [18]. The structure of B06 is shown in Fig. 1. B06 was dissolved in dimethyl sulfoxide (DMSO) for *in vitro* experiments and was dissolved in 1% CMC-Na for *in vivo* experiments. Anti-β-actin antibody was purchased from Santa Cruz (Santa Cruz, CA, USA). Anti-p-inhibitor of NF-κB (IκB) α and anti-CD68 antibodies were brought from Cell Signaling (Danvers, MA, USA).

2.2. Animals

Male Sprague-Dawley (SD) rats weighting 200–250 g and Institute of Cancer Research (ICR) mice weighing 18–22 g were purchased from SLAC Laboratory Animal Center (Shanghai, China). Animals were housed at a constant room temperature with a 12:12-h light–dark cycle, and fed with a standard rodent diet and water. The animals were acclimatized to the laboratory for at least 3 days before used. All experiments complied with the Wenzhou Medical College Policy on the Care and Use of Laboratory Animals.

2.3. Diabetic induction and sample collection

Male SD rats were randomly divided into three groups: control, diabetic (DM), or diabetic treated with B06 (DM+B06). Diabetes was induced by a single intraperitoneal injection of freshly prepared STZ (65 mg/kg in citrate buffer, pH=4.5) [20]. Control animals received the same volume of citrate buffer. Three days after STZ injection, mice with whole-blood glucose ≥16.7 mM were considered

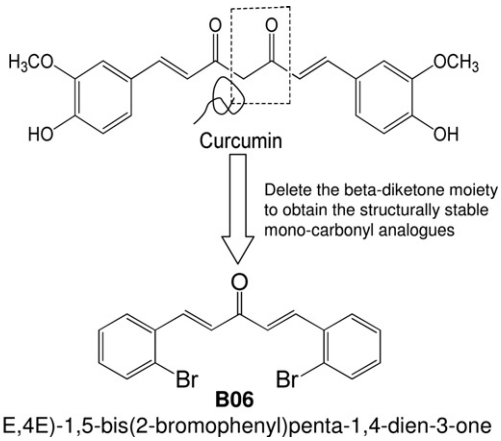

Fig. 1. Chemical structures of curcumin and B06.

diabetic. Seven days after STZ treatment, B06 dissolved in 1% CMC-Na was given by gavage at the dosage of 0.2 $mg \cdot kg^{-1} \cdot d^{-1}$ for 6 weeks. Control mice received 1% CMC-Na alone in the same schedule as the B06 treatment group. Body weights were checked weekly, and blood glucose was measured at days 7, 9, 16, 22, 40, and 49 after STZ induction. Seven weeks after STZ induction, the rats were killed under ether anesthesia, and blood was collected from the right ventricle using a heparinized syringe with a needle. At the same time, the hearts and kidneys were harvested and weighed. Serum glucose, TNF-α, nitrite levels, and creatinine levels were determined by an automatic biochemical analyzer.

2.4. Pathological analysis

Hearts and kidneys from SD rats were fixed in 4% paraformaldehyde and embedded in paraffin. The paraffin sections (5 μm) were stained with hematoxylin and eosin (H&E) for histopathological observation, with 0.5% periodic acid and Schiff solution (PAS) for glycogen analysis or with 0.1% Sirius red F3B and 1.3% saturated aqueous solution of picric acid for the analysis of type IV collagen collection. The specimens were observed under a light or fluorescent microscope (×400; Nikon, Tokyo, Japan).

2.5. Immunohistochemistry

After deparaffinization and rehydration, slides with 5-μm kidney sections were treated with 3% H_2O_2 for 10 min and with 1% bovine serum albumin in phosphate-buffered saline (PBS) for 30 min. Slides were incubated overnight at 4°C with anti-CD68 antibody (1:50), then incubated with fluorescent isothiocyanate-labeled secondary antibody (Santa Cruz Biotechnology, Santa Cruz, CA, USA; 1:500) for 1 h at room temperature. After the nuclei were stained with DAPI for 5 min, the images were viewed by a fluorescent microscope (×400).

2.6. Preparation of mouse peritoneal macrophages and in vitro culture and treatment

ICR mice were stimulated by intraperitoneal injection of 6% thioglycollate solution (0.3 g beef extract, 1 g tryptone, 0.5 g sodium chloride dissolved in 100 ml ddH_2O, and filtrated through 0.22-μm filter membrane, 3 ml per mouse) and kept in a pathogen-free condition for 3 days before mouse peritoneal macrophages (MPMs) isolation. Total MPMs were harvested by washing the peritoneal cavity with PBS containing 30 mM of EDTA (8 ml per mouse), centrifuged, and suspended in RPMI-1640 medium (Gibco/BRL life Technologies, Eggenstein, Germany) with 10% fetal bovine serum (Hyclone, Logan, UT, USA), 100 U/ml penicillin, and 100 mg/ml streptomycin. Nonadherent cells were removed by washing with medium 3 h after seeding. Experiments were undertaken after the cells were firmly adhered to the culture plates. Before treatment, MPMs were cultured in 60-mm plates (1.2×10^6 cells per plate with 3 ml PRMI-1640 medium) and incubated overnight at 37°C in a 5% CO_2-humidified air. After overnight incubation, cells were treated with 2.5 or 5 μM B06 for 2 h and then incubated with HG (25 mmol/L D-glucose) or low glucose (LG; 5.5 mmol/L D-glucose) for 3 or 18 h. The collected culture-conditioned medium was centrifuged, and the supernatant was stored at −80°C before analysis. The collected MPMs were detached for extraction of RNA.

2.7. Determination of TNF-α and IL-6

The TNF-α and IL-6 levels in cell medium or plasma from SD rats for diabetes study were determined with an enzyme-linked immunosorbent assay kit (Bioscience, San Diego, CA, USA) according to the manufacturer's instructions. The

Table 1
Sequences of the primers used for this study

Source	Gene	Sequence 5′–3′ (forward)	Sequence 5′–3′ (reverse)
Mouse	*TNF-α*	TGGAACTGGCAGAAGAGG	AGACAGAAGAGCGTGGTG
	IL-6	GAGGATACCACTCCCAACAGACC	AAGTGCATCATCGTTGTTCATACA
	COX-2	TGGTGCCTGGTCTGATGATG	GTGGTAACCGCTCAGGTGTTG
	iNOS	CAGCTGGGCTGTACAAACCTT	CATTGGAAGTGAAGCGTTTCG
	IL-1β	ACTCCTTAGTCCTCGGCCA	CCATCAGAGGCAAGGAGGAA
	IL-12	GGAAGCACGGCAGCAGAATA	AACTTGAGGGAGAAGTAGGAATGG
	β-Actin	TGGAATCCTGTGGCATCCATGAAAC	TAAAACGCAGCTCAGTAACAGTCCG
Rat	*TNF-α*	TACTCCCAGGTTCTCTTCAAGG	GGAGGCTGACTTTCTCCTGGTA
	TGF-β	GCAACAACGCAATCTATGAC	CCTGTATTCCGTCTCCTT
	MCP-1	GTCACCAAGCTCAAGAGAGAGA	GAGTGGATGCATTAGCTTCAGA
	iNOS	AGGCCACCTCGGATATCTCT	GCTTGTCTCTGGGTCCTCTG
	COX-2	CGGAGGAGAAGTGGGGTTTAGGAT	TGGGAGGCACTTGCGTTGATGG
	β-Actin	AAGTCCCTCACCCTCCCAAAAG	AAGCAATGCTGTCACCTTCCC

total amounts of TNF-α and IL-6 in the cell medium were normalized to the total protein amount of the viable cell pellets. Experiments were performed at least three times and in duplicate.

2.8. Nitrite release assay

Samples (100 μl) from tissues of the kidney and heart and plasma in rats for diabetes studies or MPMs were collected and combined with 50 μl 1% sulfanilamide in 5% H_3PO_4 and 50 μl 0.1% *N*-(1-naphthyl)ethylenediamine dihydrochloride (Sigma, Louis, MO, USA) in water in a 96-well plate, followed by spectrometric measurement at 550 nm with a microplate reader (MD, Sunnyvale, CA, USA). Nitrite concentration in the supernatant was determined against standard curve of a sodium nitrite.

2.9. RNA extraction and real-time quantitative polymerase chain (RT-qPCR)

Cells or kidney tissues (50–100 mg) were homogenized in TRIzol (Invitrogen, Carlsbad, CA, USA) for extraction of RNA according to manufacturer's protocol. Both reverse transcription and quantitative PCR were carried out using a two-step M-MLV Platinum SYBR Green qPCR SuperMix-UDG kit (Invitrogen, Carlsbad, CA, USA). Eppendorf Mastercycler ep realplex detection system (Eppendorf, Hamburg, Germany) was used for RT-qPCR analysis. The primers of genes including iNOS, COX-2, TNF-α, IL-6, IL-1β, IL-12, TGF-β, MCP-1, and β-actin were synthesized from Invitrogen (Shanghai, China). The primer sequences used were listed in Table 1. The amount of each gene was determined and normalized to the amount of β-actin.

2.10. Western blotting analysis

The MPMs were harvested and lysated for protein isolation. Thirty micrograms of protein was separated by 10% sodium dodecyl sulfate-polyacrylamide gel electrophoresis and electrotransferred to a nitrocellulose membrane. Each membrane was preincubated for 1 h at room temperature in Tris-buffered saline, pH 7.6, containing 0.05% Tween 20 and 5% nonfat milk. Each nitrocellulose membrane was incubated with specific antibodies. Immunoreactive bands were then detected by incubating with secondary antibody conjugated with horseradish peroxidase and visualized using enhanced chemiluminescence reagents (Bio-Rad, Hercules, CA, USA). The amounts of the proteins were analyzed using Image J analysis software version 1.38e and normalized with their respective control.

2.11. Assay of cellular NF-κB p-65 translocation

MPMs were immunofluorescence labeled according to the manufacturer's instruction using a Cellular NF-κB p65 Translocation Kit (Beyotime Biotech, Nantong, China). p65 protein and nuclei fluoresce red and blue, respectively, can be simultaneously viewed by fluorescence microscope (×200; Nikon) at an excitation wavelength of 350 nm for DAPI and 540 nm for Cy3. To create a two-color image, the red and blue images were overlaid. Experiments were performed at least three times and in duplicate.

2.12. Statistical analysis

Data were collected from repeated experiments and were presented as mean ±SEM. Student's *t* test and analysis of variance statistical software in GraphPad Pro (GraphPad, San Diego, CA, USA) were used for analyzing the differences between sets of data. Differences were considered to be significant at $P<.05$.

3. Results

3.1. B06 reduced the production of TNF-α, IL-6, and nitrite from HG-stimulated MPMs

To determine the preventive effects of B06 on HG-induced inflammation, we examined whether B06 could inhibit HG-induced increases of TNF-α, IL-6, and nitrite in *in vitro* MPMs. The MPMs were pretreated with B06 (2.5 or 5 μl) or DMSO for 2 h and then incubated with either LG (5.5 mM D-glucose) or HG (25 mM D-glucose) for 18 h. Mannitol (25 mM) was used as the control to exclude the interference of the high-osmotic condition. As shown in Fig. 2, HG stimulation significantly increased the expression of TNF-α (Fig. 2A) and IL-6 (Fig. 2B) and the production of nitrite (Fig. 2C), while treatment with B06 at indicated concentrations significantly inhibited these increases

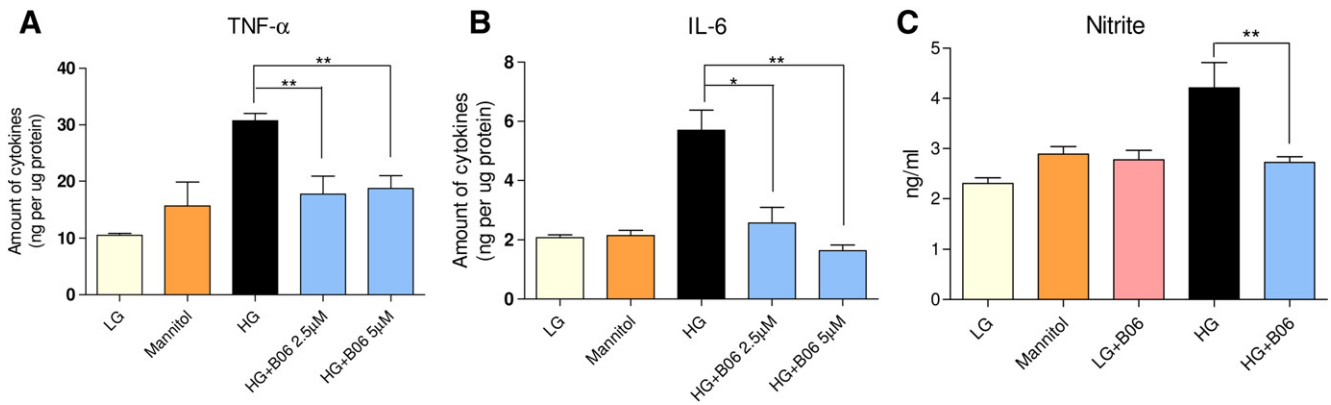

Fig. 2. B06 inhibited HG-induced TNF-α, IL-6, and nitrite production. MPMs (1×10^6) were pretreated with B06 (2.5 or 5 μM) or vehicle (DMSO, 3 μl) for 2 h and then stimulated with LG (5.5 mM), mannitol (25 mM), or HG (25 mM) for 18 h. The levels of TNF-α (A), IL-6 (B), and nitrite (C) in the medium were detected as described in Methods and materials. Bars represent the mean±SEM of three independent experiments performed in duplicate, and asterisks indicate significant inhibition ($^*P<.05$, $^{**}P<.01$ vs. the HG group).

($P<.01$). Also, Fig. 2 shows that treatment with mannitol did not change the TNF-α, IL-6, and nitrite profiles, suggesting that HG-stimulated the generation of inflammatory cytokines was not due to the osmotic change. These data show that B06 exhibited a strong inhibitory effect on HG-stimulated inflammatory responses in MPMs.

3.2. Mechanistic studies on the anti-inflammatory effect of B06 in MPMs

3.2.1. B06 significantly inhibited HG-induced inflammatory gene expression in MPMs

Then, we wanted to define whether the inhibitory effects of B06 against HG-induced protein generation of TNF-α and IL-6 are due to its inhibition at transcriptional levels and, if so, whether HG also affects other inflammatory cytokines such as IL-12, IL-1β, COX-2, and iNOS, which are representative and important in the pathogenesis of inflammatory complications [3–7]. MPMs with and without pretreatment with B06 were exposed to LG or HG for 3 h. Analysis of the cytokine messenger RNA (mRNA) expression, measured using RT-qPCR, showed that HG induced significant increases in not only TNF-α (Fig. 3B) and IL-6 (Fig. 3D) but also others such as IL-12 (Fig. 3A), IL-1β (Fig. 3C), COX-2 (Fig. 3E), and iNOS (Fig. 3F). However, B06 at 5 μM significantly decreased the HG-stimulated expression of all these inflammatory cytokines at mRNA levels (Fig. 3, $P<.01$). These data confirm that B06 treatment could alter a series of HG-induced inflammatory gene overexpression at the mRNA levels, which may be mediated by its down-regulation of an upstream transcriptional factor that controls inflammatory cytokines.

3.2.2. B06 suppressed HG-induced JNK/NF-κB signaling activation in MPMs

It is well known that NF-κB, as a nuclear transcriptional factor, plays a key role in regulating immune and inflammation. Thus, the next study was to define the effect of B06 on NF-κB signaling. Since the phosphorylation and degradation of IκB play important roles in mediating the activation of NF-κB [21,22], we first evaluated the effects of B06 on IκB phosphorylation and degradation in HG-stimulated MPMs. As shown in Fig. 4, exposure of MPMs to HG for 30 min significantly increased IκBα phosphorylation at Ser 32/36 (Fig. 4A, C) and degradation (Fig. 4B, C), and pretreatment with B06 at 5 μM markedly reduced HG-induced IκB phosphorylation and IκB degradation. Fig. 4D–G further shows that HG can accelerate NF-κB p65 translocation from cytoplasm to nuclei (red for p65 and blue for nuclei), whereas in the B06-pretreated cells, the amounts of nuclear p65 units were significantly reduced.

JNK has been demonstrated as an upstream regulator of NF-κB signal [22,23]. We tested whether the anti-inflammatory effect and NF-κB signaling inactivation of B06 are due to its interference with JNK pathway. Fig. 4H shows that HG also stimulated phosphorylation of JNK, and this effect can be completely prevented by pretreatment with B06. These data suggest that B06 inhibition of HG-induced inflammatory and NF-κB signaling activation may be associated with its suppression of JNK activation.

3.3. B06 prevented diabetic renal and cardiac pathogenic changes probably via its suppression of diabetic inflammatory stress

3.3.1. B06 did not significantly affect blood glucose level and body weight gain of diabetic rats

Diabetes was induced in rats by a single intraperitoneal injection of freshly prepared STZ, and significantly increased blood glucose level (Fig. 5A) and decreased body weight gain (Fig. 5B) were observed in diabetic rats compared to control animals, consistent with our previous studies [24–26]. Treatment with B06 did not significantly affect these parameters, suggesting that B06 at the

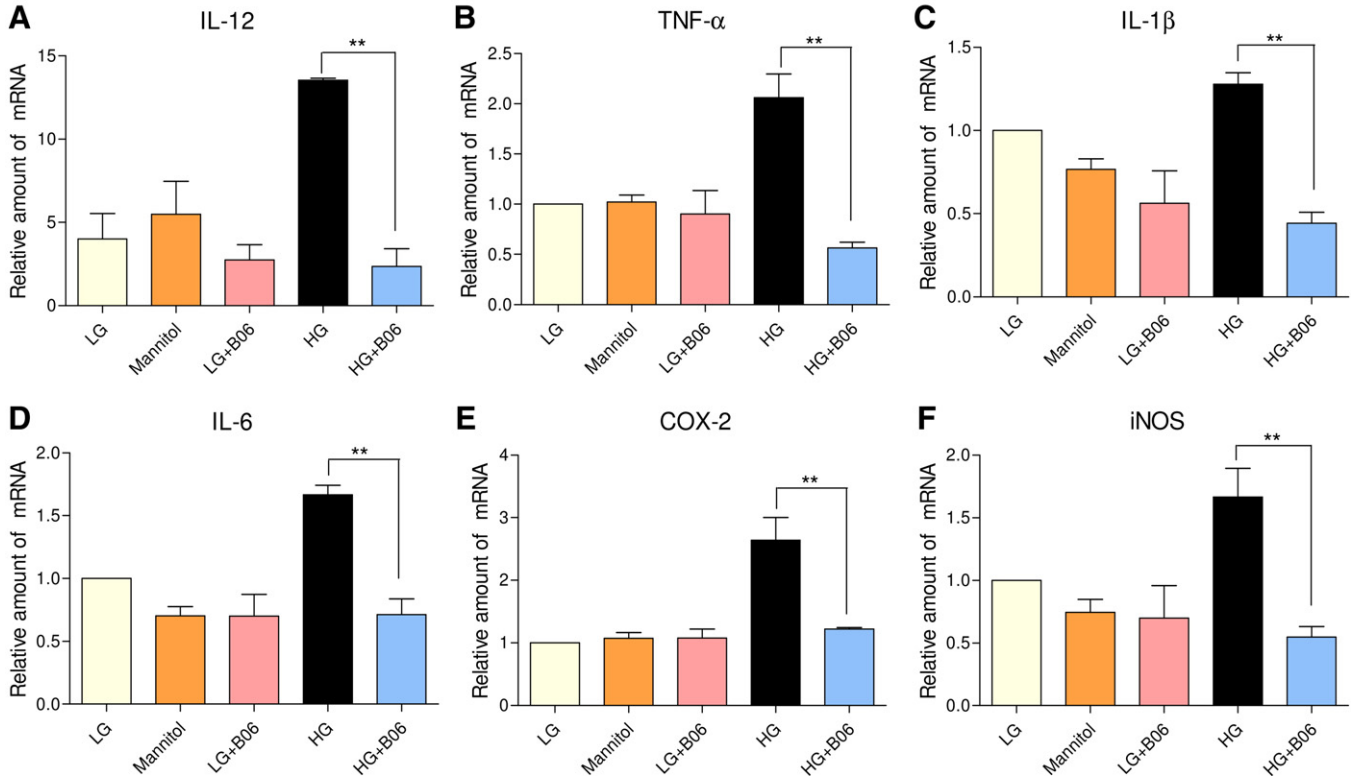

Fig. 3. B06 inhibited HG-induced inflammatory mRNA expression in MPMs. MPMs (1×10^6) were pretreated with B06 (5 μM) or vehicle (DMSO, 3 μl) for 2 h and then stimulated with LG (5.5 mM), mannitol (25 mM), or HG (25 mM) for 3 h. The mRNA levels of IL-12 (A), TNF-α (B), IL-1β (C), IL-6 (D), COX-2 (E), and iNOS (F) were detected by RT-qPCR as described in Methods and materials. Bars represent the mean±SEM of three independent experiments performed in duplicate, and asterisks indicate significant inhibition (*$P<.05$, **$P<.01$ vs. the HG group).

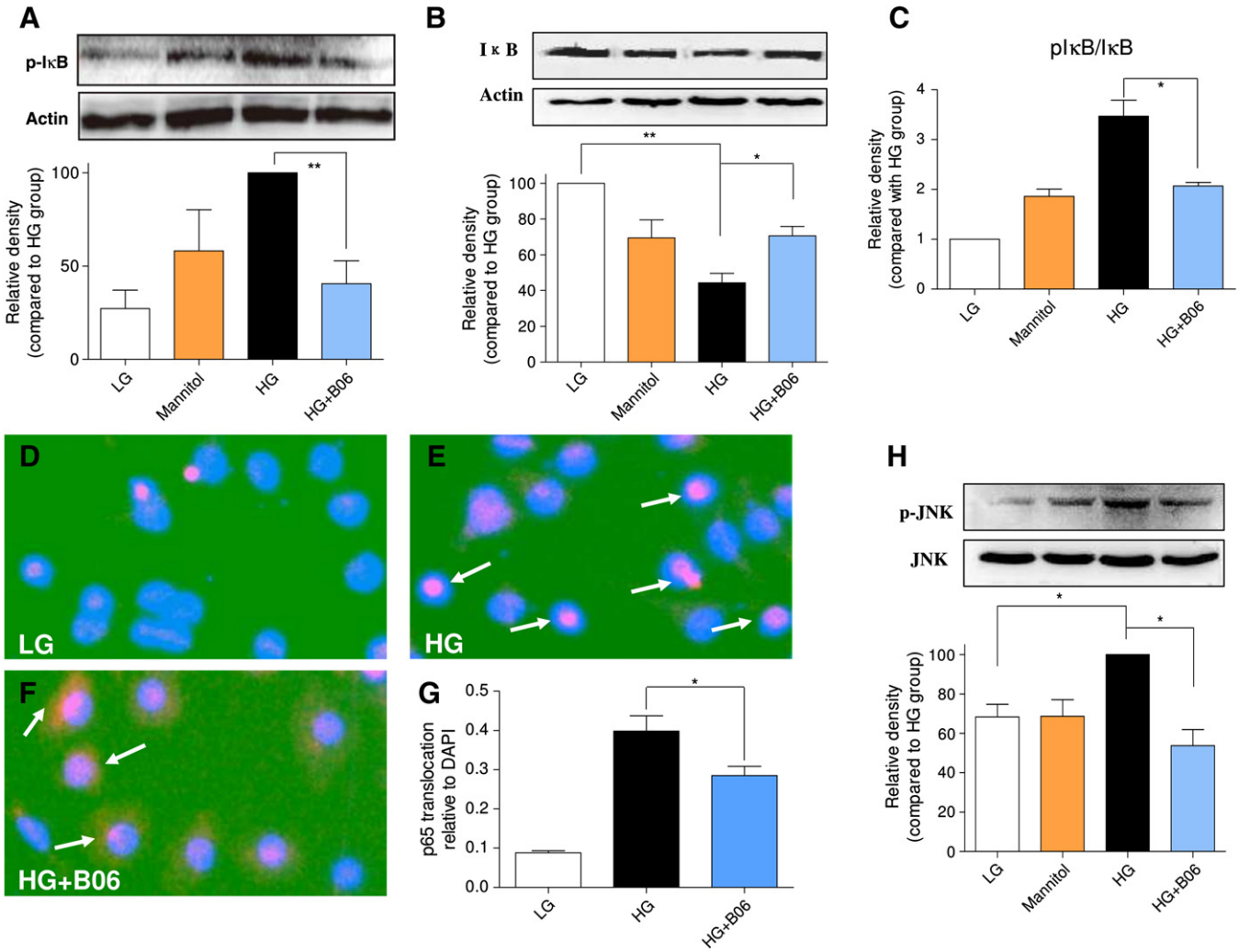

Fig. 4. B06 inhibited HG-induced NF-κB/JNK activation in MPMs. MPMs were pretreated with B06 (5 μM) or vehicle (DMSO, 3 μl) for 2 h and then stimulated with LG (5.5 mM), mannitol (25 mM), or HG (25 mM) for 30 min. The levels of p-IκB (A), IκB (B), p-IκB/IκB ratio (C), and p-JNK (H) were examined using specific antibodies with actin or total JNK as the loading control, respectively. The column figures show the normalized optical density as percentage of HG group. Bars represent the mean±SEM of four independent experiments (**P<.01 vs. the HG group). (D–F) MPMs were pretreated with B06 (5 μM) or vehicle (DMSO, 3 μl) for 2 h and then stimulated with LG (5.5 mM) or HG (25 mM) for 4 h. An immunofluorescence-labeled staining for NF-κB p65 translocation was performed by the method described in Methods and materials. (G) The number of nuclear NF-κB p65-positive cells was counted in four vision fields of 100-μm length across the culture plate. Bars represent the mean±SEM of three independent experiments (**P<.01 vs. the HG group).

dosage of 0.2 $mg \cdot kg^{-1} \cdot d^{-1}$ did not affect the diabetic model (Fig. 5A, B).

3.3.2. B06 reduced diabetes-induced pathogenic changes of the kidney and heart in the rat model

Since inflammatory response is a critical cause of diabetic complications and B06 exhibited a potent anti-inflammatory property, we hypothesized that it may protect against diabetes-induced pathogenic changes in the kidney and heart. For the kidney, the increase of the plasma creatinine level as one of renal dysfunctions was observed in the diabetic rats but not in the diabetic rats with B06 treatment at the sixth week after diabetes onset (Fig. 5C). In line with the finding in Fig. 5C, the significant increases in kidney weight/body weight ratio as a marker of renal damage was also evident in diabetic rats but not in the diabetic rats with B06 treatment (Fig. 5D).

Next, the histopathology of the kidney and heart was examined to determine the effect of B06 at 0.2 $mg \cdot kg^{-1} \cdot d^{-1}$ on diabetes-induced pathological damage to these organs. Renal staining with H&E exhibited that glomerular expansion, mesangial matrix expansion, and inflammatory cell infiltration occurred in the diabetic group (Fig. 6B), while these diabetes-induced histopathological alterations were not evident in the control (Fig. 6A) and B06-treated groups (Fig. 6C). Similarly, PAS staining showed a significant increase in PAS-positive materials (purple plaques) as indication of glycogen accumulation in diabetic glomeruli (Fig. 6E) but not in the control (Fig. 6D) and B06-treated diabetic glomeruli (Fig. 6F, J). Furthermore, renal accumulation of collagen type IV in the diabetic groups was confirmed by Sirius red staining (Fig. 6G–I). In the control kidneys, collagen was seldom detected (Fig. 6G), while in the diabetic kidneys (Fig. 6H), numerous collagens (red plaques) were observed. B06 treatment significantly attenuated the collagen accumulation in DM+B06 group (Fig. 6I, K).

H&E staining also exhibited the significant structural damage in the heart of diabetic groups (Fig. 7). Compared with the control hearts (Fig. 7A), diabetic hearts displayed a significant disarrangement of the cardiomyocytes and necrotic foci with and without scar (Fig. 7B), but these abnormalities were significantly reduced by B06 treatment for 6 weeks (Fig. 7C). PAS (Fig. 7D–F, J) and Sirius red stains (Fig. 7G–I, K) demonstrated that B06 administration significantly attenuated the diabetes-induced cardiac accumulation of glycogen and collagen.

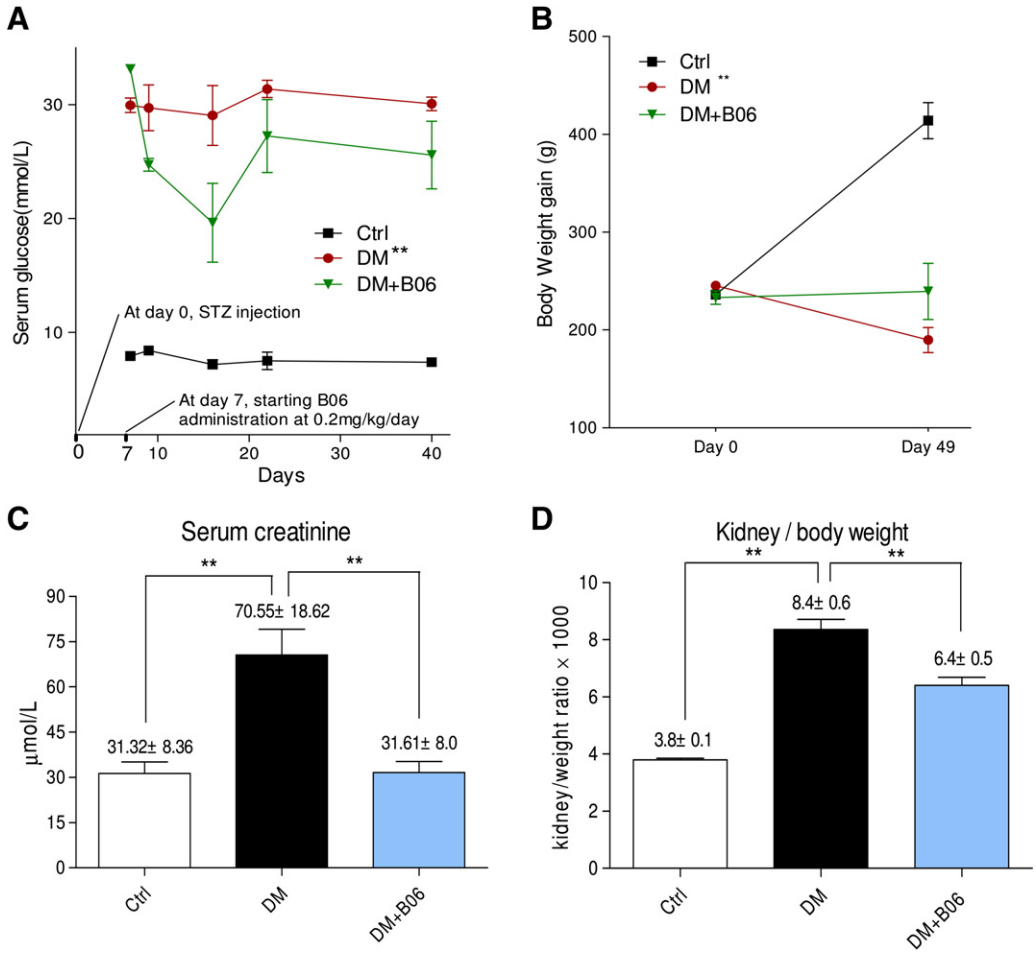

Fig. 5. The effects of B06 on the metabolic profiles of diabetic rats: serum glucose (A), body weight (B), serum creatinine (C), and kidney/body weight ratio (D). Rats and kidney samples were prepared as described in Methods and materials. The serum glucose levels were detected at indicated times. The body weight of rats was detected at the beginning of STZ induction and the time of death, respectively. Serum creatinine and kidney/body weight ratio were detected at the time of death. Data are means±SEM ($n=6$ per group; $^{**}P<.01$, DM vs. control, or DM+B06 vs. DM).

3.3.3. B06 decreased diabetes-induced inflammatory response in the rat models

The above studies indicate that B06 treatment significantly improved histological abnormalities and fibrosis in diabetic kidneys and hearts. Our next study was to define whether the renal and cardiac protection by B06 from diabetes-induced pathogenic changes is associated with B06 anti-inflammatory effect. Since the serum levels of TNF-α and nitric oxide have been accepted to reflect the degree of inflammatory response *in vivo* [3–6], we first evaluate the *in vivo* effect of B06 on serum levels of TNF-α and nitrite in diabetic rats. As shown in Fig. 8A and B, there were significant increases in serum TNF-α and nitrite in diabetic rats but not in diabetic rats with B06 at 6 weeks after diabetes onset.

In addition, the B06 prevention of renal inflammation induced by diabetes was also confirmed by determining interstitial macrophage infiltration using immunohistochemical staining for CD68 in the diabetic kidneys. Kidneys from control rats did not show significant macrophage infiltration (Fig. 8C). On the other hand, diabetic rats demonstrated prominent macrophage (CD68-positive green cells) infiltration in the glomerulus (Fig. 8D, F), while diabetic rats treated with B06 showed marked reduction of macrophage influx by 71% ($P<.01$) (Fig. 8E, F).

Next, the systemic anti-inflammatory effect by B06 was found to be accompanied by the prevention of diabetes-induced inflammatory gene expression at the organ levels. Renal and cardiac tissue mRNA transcriptions of TNF-α, COX-2, TGF-β, and MCP-1 were analyzed in parallel by RT-qPCR. Fig. 9 illustrates that all these inflammatory cytokines were significantly increased in the renal and cardiac tissues of diabetic rats but not diabetic rats with B06 treatment, suggesting that B06 could attenuate diabetes-induced cytokine expression in rat kidneys and hearts.

4. Discussion

Current therapeutics for diabetic complications mainly focuses on intensive control of glucose; however, this strategy provides imperfect protection against the progression of renal and cardiac complications associated with diabetes. Although diabetic nephropathy and cardiomyopathy traditionally have been considered to be nonimmune diseases, extensive evidence now indicates that an inflammatory mechanism may contribute to the pathogenesis of these diabetic complications [1–7,24–26]. We have demonstrated the involvement of inflammatory responses in the renal and cardiac pathogenic damage caused by diabetes [24–26]. Dalla Vestra et al. [27] also demonstrated that acute-phase markers of inflammation are associated with the severity of renal pathological changes in diabetic patients with nephropathy. Therefore, investigations into anti-inflammatory strategies may offer a new approach for mitigating diabetic inflammatory complications [28]. Anti-inflammatory agents such as *Picrorhiza scrophulariiflora* [29], retinoic acid [30], aspirin [31],

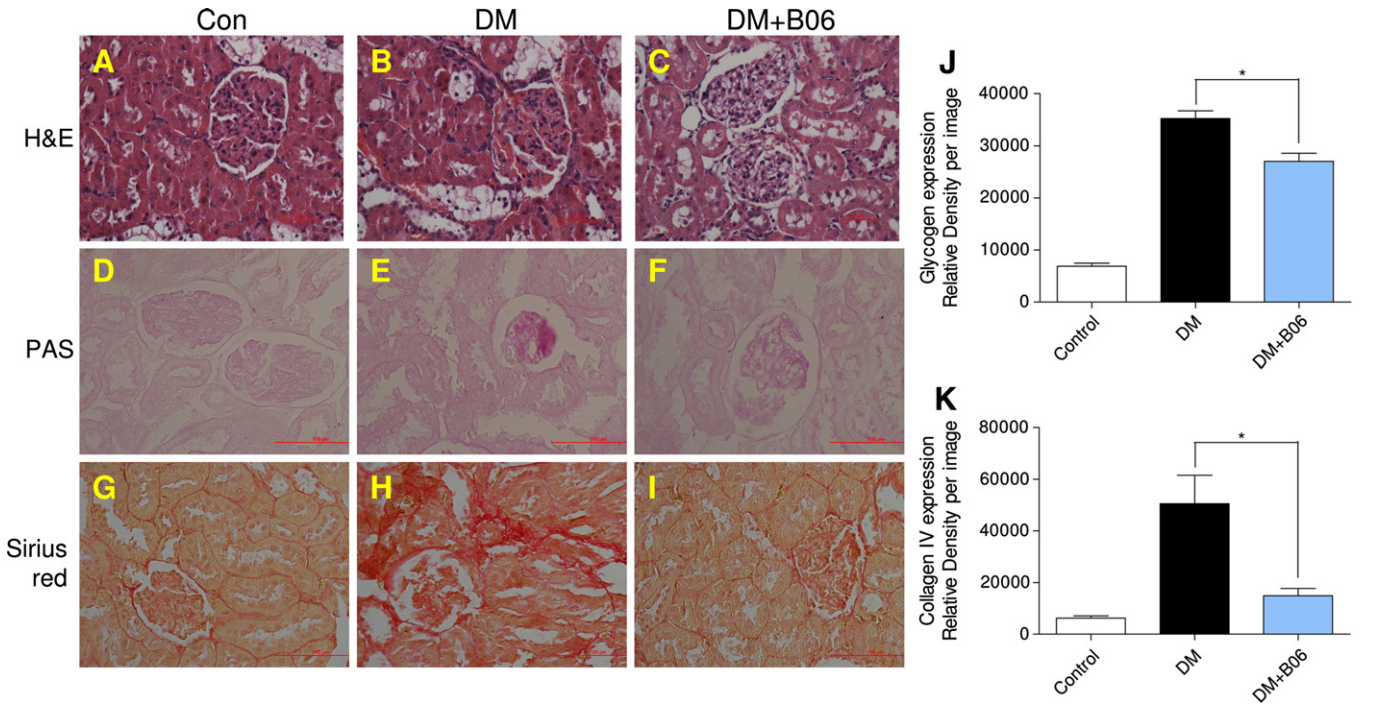

Fig. 6. B06 administration significantly improved histological abnormalities, fibrosis, and macrophage infiltration in diabetic kidney. Rats and kidney samples were prepared as described in Methods and materials. (A–C) Renal histopathological analysis was performed using H&E staining (×400). (D–F) Representative figures of PAS staining (×400) for glycogen (purple) on renal tissue (seventh week). (G–I) Representative figures of Sirius red staining (×400) for type IV collagen (red) on renal tissue (seventh week). A representative animal of six studied in each group is shown. (J) The relative density of glycogen expression per image was counted in three vision fields of 100-μm length across the kidney. Data are presented as means±SEM (*P<.05). (K) The relative density of collagen IV expression per image was counted in three vision fields of 100-μm length across the kidney. Data are presented as means±SEM (*P<.05).

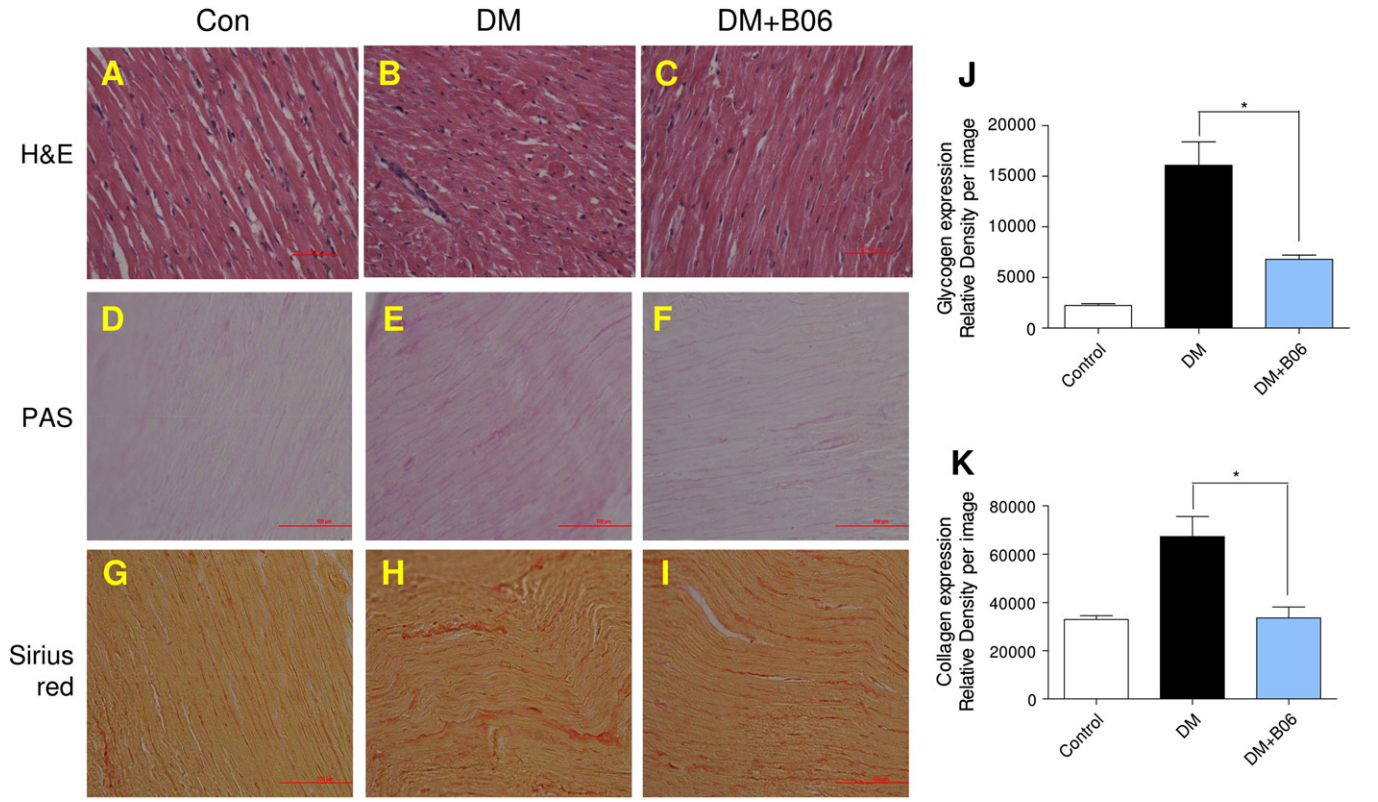

Fig. 7. B06 administration significantly improved histological abnormalities and fibrosis in diabetic heart. Rats and heart samples were prepared as described in Methods and materials. (A–C) Histopathological analysis was performed using H&E staining (×400). (D–F) Representative figures of PAS staining (×400) for glycogen (purple) on cardiac tissue (seventh week). (G–I) Representative figures of Sirius red staining (×400) for type IV collagen (red) on cardiac tissue (seventh week). A representative animal of six studied in each group is shown. (J) The relative density of glycogen expression per image was counted in three vision fields of 100-μm length across the heart. Data are presented as means±SEM (*P<.05). (K) The relative density of collagen IV expression per image was counted in three vision fields of 100-μm length across the heart. Data are presented as meas±SEM (*P<.05).

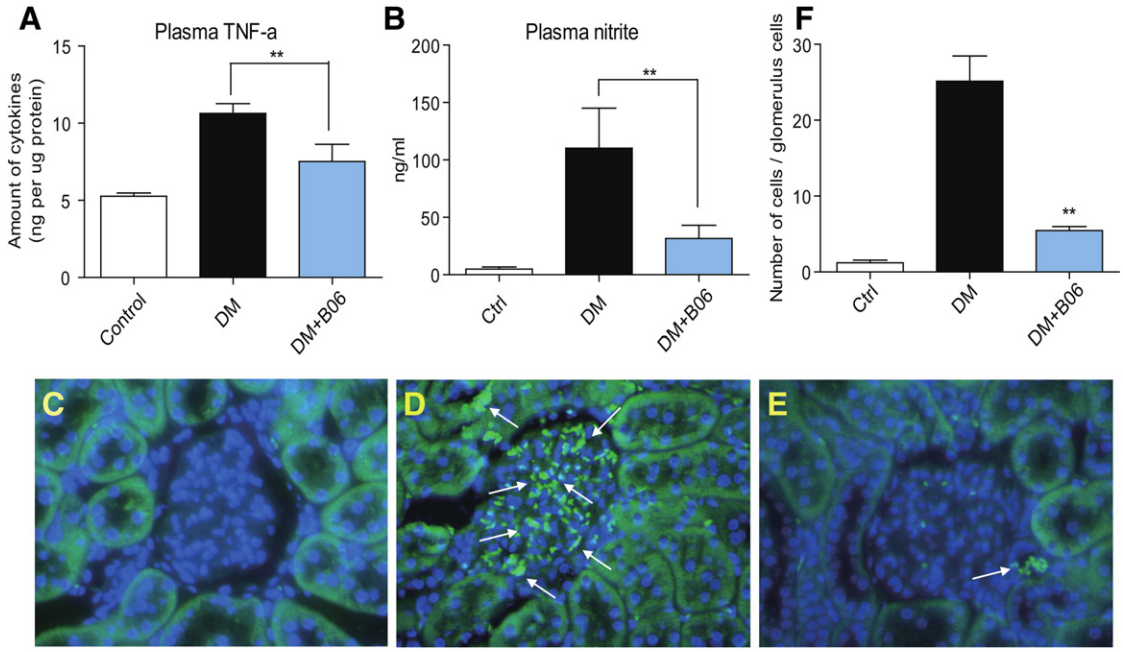

Fig. 8. B06 reduced diabetes-induced nitric oxide production and TNF-α level *in vivo*. Six weeks after B06 administration at 0.2 $mg \cdot kg^{-1} \cdot d^{-1}$, all rats in three groups were killed under ether anesthesia, and the heart, both kidneys, and blood samples were harvested. (A) TNF-α level in rat plasma ($n=6$ per group). (B) Nitrite level in rat plasma ($n=6$ per group). (C–E) Macrophage infiltration in the kidney was evaluated using anti-CD68 antibodies. Arrows indicate stained interstitial inflammatory cells (×400). A representative animal of six studied in each group is shown. (K) Quantification results are shown for number of macrophages (CD68-positive cells). (*$P<.05$ and **$P<.01$ vs. the DM group).

cannabidiol [32], resveratrol [33], and curcumin [34,35] have been reported to prevent the development of diabetic nephropathy and cardiomyopathy in animals, probably through an anti-inflammatory mechanism. Among these anti-inflammatory reagents, curcumin seems more promising in the aspect of antidiabetic inflammation due to the following facts.

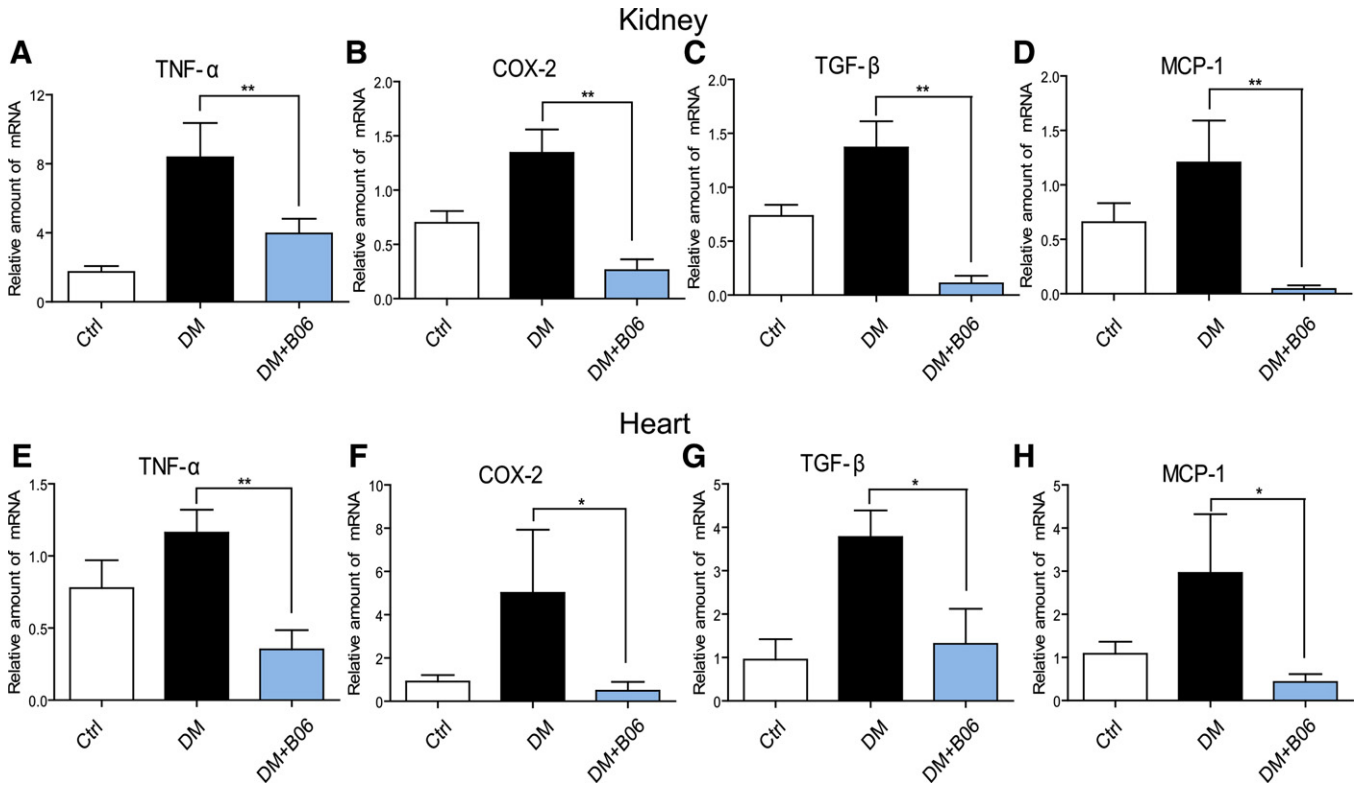

Fig. 9. Effects of B06 on inflammatory proteins in diabetic kidney (A–D) and diabetic heart (E–H). Six weeks after B06 administration at 0.2 $mg \cdot kg^{-1} \cdot d^{-1}$, all rats in three groups were killed under ether anesthesia, and the heart, both kidneys, and blood samples were harvested. The mRNA expression of TNF-α, iNOS, COX-2, TGF-β, and MCP-1 were estimated by the RT-qPCR. The mRNA expression of inflammatory genes was normalized to β-actin mRNA content. Bar graph shows mean±SEM from six rats in each group (*$P<.05$ and **$P<.01$ vs. the DM group).

Curcumin inhibits NF-κB-dependent inflammatory response *in vitro* and *in vivo* [11,36]. Independent groups have found that chronic oral administration of curcumin (50 or 150 $mg \cdot kg^{-1} \cdot d^{-1}$) significantly ameliorated renal dysfunction in diabetic rats [12,34,35]. For instance, Chiu et al. [11] reported that curcumin at a dosage of 150 $mg \cdot kg^{-1} \cdot d^{-1}$ prevented diabetes-associated abnormalities in rat kidneys by inhibiting p300 and NF-κB. Tikoo et al. [12] demonstrated that treatment of diabetic rats with curcumin at 50 $mg \cdot kg^{-1} \cdot d^{-1}$ for 6 weeks significantly increased blood urea nitrogen and creatinine and increased albumin, along with a prevention of the variables that are associated with the development of diabetic nephropathy.

However, due to the poor bioavailability of curcumin *in vivo*, high dosages are needed in animal and human studies [14,15]. A recent study of diabetic mice showed that the administration of curcumin (5000–7500 ppm in diet, equal to 200–300 $mg \cdot kg^{-1} \cdot d^{-1}$) failed to attenuate nephropathy, probably due to its poor bioavailability *in vivo* [37]. There were no clinical trials of curcumin in diabetic humans yet, and only a few clinical investigations indicated limited beneficial effect due to its instability and poor pharmacokinetic properties [14,15]. In order to improve the pharmacokinetic parameters of curcumin, a series of monocarbonyl curcumin analogues have been designed and synthesized in our previous studies [18]. A preliminary pharmacokinetic study showed that the structural modification from curcumin to B06 significantly decreased the degree and speed of metabolism of curcumin and that B06 possessed much better pharmacokinetic profiles than did curcumin [18]. B06 also significantly inhibited LPS-induced releases of TNF-α and IL-6 *in vitro* with a 1.8-fold and 2.1-fold increases over the inhibitory ability of nonmodified curcumin, respectively [19]. In addition, B06 exhibited significantly anti-inflammatory properties in HG-activated macrophages (Fig. 2). In keeping with such studies, we designed an *in vivo* dosage about 250-fold lower than that of curcumin.

In the present study, we first provide the evidence to show the potent *in vivo* anti-inflammatory and protective effects of B06 at an extremely low dosage (0.2 $mg \cdot kg^{-1} \cdot d^{-1}$) in a STZ-induced diabetic rat model. Compared with the nontreated diabetic group, treatment with B06 did not affect blood glucose level or body weight (Fig. 5A, B). However, B06 treatment significantly down-regulated the renal and cardiac pathological changes compared to nontreated diabetes (Figs. 6 and 7). These pathogenic damage to the kidney and heart is associated with systemic and organ's anti-inflammatory effect. As the major immune cells, macrophage accumulation contributes to the development of renal injury and sclerosis [38]. Also, we observed that the systemic administration of B06 in diabetic rats decreases the glomerular infiltration of macrophages (Fig. 8C–E). The H&E staining results shown in Fig. 6A–C further supported that B06 treatment reduced renal and cardiac infiltration of leukocytes, including macrophages. Our data also demonstrated that B06 inhibited the expression of MCP-1 and TNF-α in diabetic kidneys and hearts (Fig. 9), suggesting the possible mechanism for the suppression of macrophage infiltration. Together, our *in vivo* data clearly show that B06 attenuates inflammatory factors and decreases macrophage accumulation in diabetic rats.

The protective action of B06 against HG- or diabetes-induced inflammation attributes to its multiorgan protective action in diabetic rats. *In vitro*, our results demonstrated that the HG-stimulated increase of cytokine mRNA transcriptions was not elicited by mannitol-induced high-osmotic condition, indicating that HG induces inflammation via a classic transcriptional or posttranscriptional mechanism. In the present study, we demonstrated the inhibitory effects of B06 on mRNA and protein expressions of inflammatory cytokines induced by HG in MPMs (Figs. 2 and 3), which was also supported by the *in vivo* model that B06 pretreatment significantly prevented the renal and cardiac inflammation and inflammatory gene expressions (Figs. 8 and 9).

Among the intracellular signaling systems involved in the regulation of inflammatory and immune responses, JNK/NF-κB is of special interest. Curcumin has been identified as an inhibitor for JNK/NF-κB-dependent inflammation *in vitro* and *in vivo* [9], and it also reduces HG-induced inflammatory gene expression by modulating the NF-κB pathway [5]. The phosphorylation and dissociation of IκB from the inactive cytosolic complex lead to the translocation of the active subunit NF-κB p65 from the cytosolic to nuclear fractions, which binds to the DNA sites and triggers gene expressions [21,22]. JNK has been demonstrated as an upstream regulator of NF-κB signal [22]. In macrophages, HG causes a significant JNK phosphorylation that activates the NF-κB signal [39]. Our results, shown in Fig. 4, suggest that B06 inactivates JNK/NF-κB signaling by inhibiting JNK phosphorylation, IκB phosphorylation and degradation, and p65 translocation, indicating that the anti-inflammatory actions of B06 are associated with transcriptional suppression on the NF-κB pathway via suppressing JNK pathway. However, it is unclear whether the inflammatory inhibition of B06 is JNK/NF-κB dependent. In addition, although many curcumin beneficial effects have been found to be due to its inhibition of JNK/NF-κB and the subsequent inhibition of proinflammatory pathways, its molecular target for direct binding is still unknown. Therefore, although this work only focuses on the JNK/NF-κB-mediated inflammation, further studies are necessary to establish such notion as examination of the underlying molecular mechanisms and direct molecular targets of B06.

The findings reported here support the possibility that the novel curcumin analogue, B06, inhibits the proinflammatory mediators at the transcriptional level and subsequently attenuates the inflammatory process and pathological dysfunction in diabetic kidneys and hearts. Compared to curcumin, B06 has both pharmacological and pharmaceutical advantages. It exerts a beneficial effect on diabetic inflammation and multiorgan damage at an extremely low dosage of 0.2 $mg \cdot kg^{-1} \cdot d^{-1}$. In a preliminary safety assay in our laboratory, all ICR mice survived in a 14-day observation after being treated with B06 at 1000 mg/kg (data not shown). These results strongly suggest that the novel compound, B06, is a potential agent for the treatment of diabetic complications via an anti-inflammatory mechanism. This study also supports the potential application in diabetic complication therapy via anti-inflammatory strategy.

Acknowledgments

This study was supported, in part, by the National Natural Science Funding of China (81072683, 81102452, and 30971406), High-level Innovative Talent Funding of Zhejiang Department of Health (X. L. and G. L.), Project of Wenzhou Science and Technology Bureau (Y20090009 and Y20100006), and Zhejiang Natural Science Funding (Y20101108).

References

[1] Donath MY, Shoelson SE. Type 2 diabetes as an inflammatory disease. Nat Rev Immunol 2011;11:98–107.
[2] Goldfine AB, Fonseca V, Shoelson SE. Therapeutic approaches to target inflammation in type 2 diabetes. Clin Chem 2011;57:162–7.
[3] Navarro-Gonzalez JF, Mora-Fernandez C, de Fuentes MM, Garcia-Perez J. Inflammatory molecules and pathways in the pathogenesis of diabetic nephropathy. Nat Rev Nephrol 2011;7:327–40.
[4] Pickup JC. Inflammation and activated innate immunity in the pathogenesis of type 2 diabetes. Diabetes Care 2004;27:813–23.
[5] Panicker SR, Kartha CC. Curcumin attenuates glucose-induced monocyte chemoattractant protein-1 synthesis in aortic endothelial cells by modulating the nuclear factor-kappaB pathway. Pharmacology 2010;85:18–26.
[6] Lee YJ, Kang DG, Kim JS, Lee HS. Effect of Buddleja officinalis on high-glucose-induced vascular inflammation in human umbilical vein endothelial cells. Exp Biol Med (Maywood) 2008;233:694–700.
[7] Mariappan N, Elks CM, Sriramula S, Guggilam A, Liu Z, Borkhsenious O, et al. NF-kappaB-induced oxidative stress contributes to mitochondrial and cardiac dysfunction in type II diabetes. Cardiovasc Res 2010;85:473–83.

[8] Komers R, Lindsley JN, Oyama TT, Anderson S. Cyclo-oxygenase-2 inhibition attenuates the progression of nephropathy in uninephrectomized diabetic rats. Clin Exp Pharmacol Physiol 2007;34:36–41.
[9] Hanai H, Sugimoto K. Curcumin has bright prospects for the treatment of inflammatory bowel disease. Curr Pharm Des 2009;15:2087–94.
[10] Aggarwal BB, Sundaram C, Malani N, Ichikawa H. Curcumin: the Indian solid gold. Adv Exp Med Biol 2007;595:1–75.
[11] Chiu J, Khan ZA, Farhangkhoee H, Chakrabarti S. Curcumin prevents diabetes-associated abnormalities in the kidneys by inhibiting p300 and nuclear factor-kappaB. Nutrition 2009;25:964–72.
[12] Tikoo K, Meena RL, Kabra DG, Gaikwad AB. Change in post-translational modifications of histone H3, heat-shock protein-27 and MAP kinase p38 expression by curcumin in streptozotocin-induced type I diabetic nephropathy. Br J Pharmacol 2008;153:1225–31.
[13] Anand P, Kunnumakkara AB, Newman RA, Aggarwal BB. Bioavailability of curcumin: problems and promises. Mol Pharm 2007;4:807–18.
[14] Sharma RA, Euden SA, Platton SL, Cooke DN, Shafayat A, Hewitt HR, et al. Phase I clinical trial of oral curcumin: biomarkers of systemic activity and compliance. Clin Cancer Res 2004;10:6847–54.
[15] Dhillon N, Aggarwal BB, Newman RA, Wolff RA, Kunnumakkara AB, Abbruzzese JL, et al. Phase II trial of curcumin in patients with advanced pancreatic cancer. Clin Cancer Res 2008;14:4491–9.
[16] Padhye S, Chavan D, Pandey S, Deshpande J, Swamy KV, Sarkar FH. Perspectives on chemopreventive and therapeutic potential of curcumin analogs in medicinal chemistry. Mini Rev Med Chem 2010;10:372–87.
[17] Agrawal DK, Mishra PK. Curcumin and its analogues: potential anticancer agents. Med Res Rev 2010;30:818–60.
[18] Liang G, Shao LL, Wang Y, Zhao CG, Chu YH, Xiao J, et al. Exploration and synthesis of curcumin analogues with improved structural stability both in vitro and in vivo as cytotoxic agents. Bioorg Med Chem 2009;17:2623–31.
[19] Liang G, Li XK, Chen L, Yang SL, Wu XP, Studer E, et al. Synthesis and anti-inflammatory activities of mono-carbonyl analogues of curcumin. Bioorg Med Chem Lett 2008;18:1525–9.
[20] Yozai K, Shikata K, Sasaki M, Tone A, Ohga S, Usui H, et al. Methotrexate prevents renal injury in experimental diabetic rats via anti-inflammatory actions. J Am Soc Nephrol 2005;16:3326–38.
[21] Adli M, Merkhofer E, Cogswell P, Baldwin AS. IKKalpha and IKKbeta each function to regulate NF-kappaB activation in the TNF-induced/canonical pathway. PLoS One 2010;5:e9428.
[22] Jeon KI, Xu X, Aizawa T, Lim JH, Jono H, Kwon DS, et al. Vinpocetine inhibits NF-kappaB-dependent inflammation via an IKK-dependent but PDE-independent mechanism. Proc Natl Acad Sci U S A 2010;107:9795–800.
[23] Cho JW, Lee KS, Kim CW. Curcumin attenuates the expression of IL-1beta, IL-6, and TNF-alpha as well as cyclin E in TNF-alpha-treated HaCaT cells; NF-kappaB and MAPKs as potential upstream targets. Int J Mol Med 2007;19:469–74.
[24] Rane MJ, Song Y, Jin S, Barati MT, Wu R, Kausar H, et al. Interplay between Akt and p38 MAPK pathways in the regulation of renal tubular cell apoptosis associated with diabetic nephropathy. Am J Physiol Renal Physiol 2010;298:F49–61.
[25] Zhang C, Tan Y, Guo W, Li C, Ji S, Li X, et al. Attenuation of diabetes-induced renal dysfunction by multiple exposures to low-dose radiation is associated with the suppression of systemic and renal inflammation. Am J Physiol Endocrinol Metab 2009;297:E1366–77.
[26] Wang Y, Feng W, Xue W, Tan Y, Hein DW, Li XK, et al. Inactivation of GSK-3beta by metallothionein prevents diabetes-related changes in cardiac energy metabolism, inflammation, nitrosative damage, and remodeling. Diabetes 2009;58:1391–402.
[27] Dalla Vestra M, Mussap M, Gallina P, Bruseghin M, Cernigoi AM, Saller A. Acute-phase markers of inflammation and glomerular structure in patients with type 2 diabetes. J Am Soc Nephrol 2005;16(Suppl. 1):S78–82.
[28] Decleves AE, Sharma K. New pharmacological treatments for improving renal outcomes in diabetes. Nat Rev Nephrol 2010;6:371–80.
[29] He LJ, Liang M, Hou FF, Guo ZJ, Xie D, Zhang X. Ethanol extraction of Picrorhiza scrophulariiflora prevents renal injury in experimental diabetes via anti-inflammation action. J Endocrinol 2009;200:347–55.
[30] Han SY, So GA, Jee YH, Han KH, Kang YS, Kim HK, et al. Effect of retinoic acid in experimental diabetic nephropathy. Immunol Cell Biol 2004;82:568–76.
[31] Pignone M, Williams CD. Aspirin for primary prevention of cardiovascular disease in diabetes mellitus. Nat Rev Endocrinol 2010;6:619–28.
[32] Rajesh M, Mukhopadhyay P, Batkai S, Patel V, Saito K, Matsumoto S, et al. Cannabidiol attenuates cardiac dysfunction, oxidative stress, fibrosis, and inflammatory and cell death signaling pathways in diabetic cardiomyopathy. J Am Coll Cardiol 2010;56:2115–25.
[33] Sulaiman M, Matta MJ, Sunderesan NR, Gupta MP, Periasamy M, Gupta M. Resveratrol, an activator of SIRT1, upregulates sarcoplasmic calcium ATPase and improves cardiac function in diabetic cardiomyopathy. Am J Physiol Heart Circ Physiol 2010;298:H833–43.
[34] Jain SK, Rains J, Croad J, Larson B, Jones K. Curcumin supplementation lowers TNF-alpha, IL-6, IL-8, and MCP-1 secretion in high glucose-treated cultured monocytes and blood levels of TNF-alpha, IL-6, MCP-1, glucose, and glycosylated hemoglobin in diabetic rats. Antioxid Redox Signal 2009;11:241–9.
[35] Farhangkhoee H, Khan Z, Chen S, Chakrabarti S. Differential effects of curcumin on vasoactive factors in the diabetic rat heart. Nutr Metab 2006;3:27.
[36] Sun ZJ, Chen G, Zhang W, Hu X, Liu Y, Zhou Q, et al. Curcumin dually inhibits both mammalian target of rapamycin and nuclear factor-kappaB pathways through a crossed phosphatidylinositol 3-kinase/Akt/IkappaB kinase complex signaling axis in adenoid cystic carcinoma. Mol Pharmacol 2011;79:106–18.
[37] Ma J, Phillips L, Wang Y, Dai T, LaPage J, Natarajan R, et al. Curcumin activates the p38MPAK-HSP25 pathway in vitro but fails to attenuate diabetic nephropathy in DBA2J mice despite urinary clearance documented by HPLC. BMC Complement Altern Med 2010;10:67.
[38] Tesch GH. Macrophages and diabetic nephropathy. Semin Nephrol 2010;30:290–301.
[39] Wen Y, Gu J, Li SL, Reddy MA, Natarajan R, Nadler JL. Elevated glucose and diabetes promote interleukin-12 cytokine gene expression in mouse macrophages. Endocrinology 2006;147:2518–25.